Atmospheric Environment 202 (2019) 256–268

Contents lists available at ScienceDirect

Atmospheric Environment

journal homepage: www.elsevier.com/locate/atmosenv

Variability of black carbon mass concentrations, sub-micrometer particle number concentrations and size distributions: results of the German Ultrafine Aerosol Network ranging from city street to High Alpine locations

J. Sun[a], W. Birmili[a,b], M. Hermann[a], T. Tuch[a], K. Weinhold[a], G. Spindler[a], A. Schladitz[c,1], S. Bastian[c], G. Löschau[c], J. Cyrys[d,e], J. Gu[d,e,2], H. Flentje[f], B. Briel[f], C. Asbach[g], H. Kaminski[g], L. Ries[b], R. Sohmer[b], H. Gerwig[b], K. Wirtz[b], F. Meinhardt[b], A. Schwerin[b], O. Bath[b], N. Ma[h,a,*], A. Wiedensohler[a,**]

[a] Leibniz Institute for Tropospheric Research (TROPOS), Leipzig, Germany
[b] German Environment Agency (UBA), Dessau-Roßlau, Germany
[c] Saxon State Office for Environment, Agriculture and Geology (LfULG), Dresden, Germany
[d] Helmholtz Zentrum München(HMGU), Institute of Epidemiology II, Neuherberg, Germany
[e] University of Augsburg(UA), Wissenschaftszentrum Umwelt, Augsburg, Germany
[f] Deutscher Wetterdienst (DWD), Meteorologisches Observatorium Hohenpeißenberg, Germany
[g] Institute of Energy and Environmental Technology (IUTA), Duisburg, Germany
[h] Center for Air Pollution and Climate Change Research (APCC), Institute for Environmental and Climate Research (ECI), Jinan University, Guangzhou, 511443, China

ARTICLE INFO

Keywords:
Particle number size distribution
Black carbon
Long-term measurement
Spatial variability
Spatial clustering

ABSTRACT

This work reports the first statistical analysis of multi-annual data on tropospheric aerosols from the German Ultrafine Aerosol Network (GUAN). Compared to other networks worldwide, GUAN with 17 measurement locations has the most sites equipped with particle number size distribution (PNSD) and equivalent black carbon (eBC) instruments and the most site categories in Germany ranging from city street/roadside to High Alpine. As we know, the variations of eBC and particle number concentration (PNC) are influenced by several factors such as source, transformation, transport and deposition. The dominant controlling factor for different pollutant parameters might be varied, leading to the different spatio-temporal variations among the measured parameters. Currently, a study of spatio-temporal variations of PNSD and eBC considering the influences of both site categories and spatial scale is still missing. Based on the multi-site dataset of GUAN, the goal of this study is to investigate how pollutant parameters may interfere with spatial characteristics and site categories.

1. Introduction

Our understanding of processes and trends in the atmosphere relies, to a large extent, on experimental observations. Quantifiable atmospheric observations have included, since 1781, temperature (Winkler, 2009), visual phenomena and, more recently, solar radiation (Wild et al., 2005). Observations of aerosol optical depth in various locations have allowed a quantitative comparison of competing effects of global warming by carbon dioxide and possible cooling by aerosols (Hansen and Lacis, 1990). State-of-the-art, in-situ observations of aerosol particle properties yield information on particle number size distributions (PNSD), light scattering and absorption coefficients, as well as chemical composition. These parameters are essential to validate our picture of aerosol particle emissions, formation, and transport in the atmosphere as well as deposition. Other benefits from aerosol observations include the support of trends in direct radiative forcing as well as trends in particulate anthropogenic emissions. Due to fast, automated analytical methods, long-term observations are more readily available for aerosol physical properties.

Studies about aerosol physical parameters show that, elevated

* Corresponding author. Center for Air Pollution and Climate Change Research (APCC), Institute for Environmental and Climate Research (ECI), Jinan University, Guangzhou, 511443, China
** Corresponding author. Leibniz Institute for Tropospheric Research (TROPOS), Leipzig, Germany.
E-mail addresses: nan.ma@jnu.edu.cn (N. Ma), ali@tropos.de (A. Wiedensohler).
[1] now at: SICK Engineering GmbH, Ottendorf-Okrilla, Germany.
[2] now at: Fraunhofer Institute for Wood Research, Wilhelm-Klauditz-Institut, Braunschweig, Germany.

https://doi.org/10.1016/j.atmosenv.2018.12.029

Available online 26 December 2018

aerosol particle concentrations may result in an increased risk of health hazards (HEI, 2013; WHO, 2012; Kreyling et al., 2006; Lanzinger et al., 2016). Due to their high number concentrations and small diameters, ultrafine particles (UFP, particle diameter ≤ 100 nm) and black carbon (BC) have higher surface area per mass to absorb toxic materials than larger particles. Moreover, UFP have higher chance to penetrate deep into lungs and may translocate to the brain due to their small size (Oberdörster et al., 2009), and further cause human health hazards such as respiratory and cardiovascular diseases (Kreyling et al., 2006; Schmid and Stoeger, 2016). However, regular measurements of particle mass concentrations such as PM_{10} or $PM_{2.5}$ cannot well represent UFP and BC since they contribute only a minor fraction to particle total mass.

There have been lots of studies reporting the observation of UFP and BC in various environments around the world. However, the outcomes of these studies are difficult to compare and generalize. Firstly, most of the studies were established only for specific locations and environments. Some of them showed the aerosol particle variability on a local scale influenced by anthropogenic emissions from traffic, airport and domestic heating (Colvile et al., 2001; Hofman et al., 2016; Pérez et al., 2010; Rodríguez and Cuevas, 2007; Wåhlin et al., 2006; van Pinxteren et al., 2016). Some studies focused on the background aerosol concentration variation on a regional scale (Asmi et al., 2011; Beddows et al., 2014; Birmili et al., 2013; Putaud et al., 2010). And some investigations were conducted at remote sites and reported the background aerosol concentration in free troposphere (Birmili et al., 2010; Collaud Coen et al., 2011; Forrer et al., 2000; Griffiths et al., 2014). Secondly, short-term studies usually provide only a snapshot of the variation of aerosol particles at specific time periods, which might be significantly influenced by particular meteorological situations (Birmili et al., 2001; Mikkonen et al., 2011; von Bismarck-Osten et al., 2013) or specific emission sources (Beddows et al., 2014; Costabile et al., 2009). To obtain a full picture of the atmospheric aerosol particles in a region, a network of monitoring stations performing long-term measurements in different environments, including roadside, urban background, regional background and remote area, is needed (HEI, 2013).

In Europe, several studies have reported the concentration of aerosol particles as well as their physical and chemical properties (Cavalli et al., 2010; Putaud et al., 2010; Zanatta et al., 2016). Table 1 illustrates the existing aerosol observation networks. Compared with other observation networks, the German Ultrafine Aerosol Network (GUAN) has the most sites equipped with PNSD and equivalent black carbon (eBC) instruments and the most site categories. GUAN is a consortium of national environmental authorities and research institutes, aiming at a better understanding of atmospheric aerosol particles with regard to human particle exposure and aerosol climate effects. GUAN delivers a unique dataset worldwide, including long-term time series of PNSD and eBC at 17 observatories in different environments ranging from city street, urban background, regional background, low mountain range to High Alpine.

Most of previous studies about spatio-temporal variation of PNSD, particle number concentration (PNC) and BC focused on, a) how pollutant parameters vary with site categories within a relatively small spatial scale, in order to estimate the influencing factors of PNC and BC within a local area (Birmili et al., 2013; Dos Santos-Juusela et al., 2013; Krudysz et al., 2009; Rattigan et al., 2013); and b) how the pollutant parameters interfere with spatial scale in a large region, in order to investigate the representativeness of measurement sites (Asmi et al., 2011; Collaud Coen et al., 2013; Henne et al., 2010) or to generalize the common characteristics of parameter temporal variations for specific site categories (Brüske et al., 2011; Reche et al., 2011). However, a study about the spatio-temporal variability of PNSD and eBC considering the influences of both site categories and spatial scale is still missing. With long-term large scale multi-site-category measurements, GUAN provides us an opportunity to investigate how pollutant parameters interfere with spatial characteristics and site categories.

Table 1
Long-term atmospheric aerosol networks and infrastructure projects providing continuous particle number concentration, particle number size distribution and/or black carbon measurements.

Name	Region	Site categories	Observed period	References
GAW	Worldwide	Global or regional background	1992-	Asmi et al. (2013); Collaud Coen et al. (2013)
Particle numbers and concentrations network	United Kingdom	Urban or regional background	2000-	Jones et al. (2012); Van Dingenen et al. (2004)
Black Carbon network	United Kingdom	Urban or regional background	2006-	Butterfield et al. (2010)
ACTRIS[a]	Europe	Regional background	2006–2011 (EUSAAR) 2011-(ACTRIS)	Asmi et al. (2011); Asmi et al. (2013); Beddows et al. (2014); Collaud Coen et al. (2013); Costabile et al. (2010); Müller et al. (2011); Zanatta et al. (2016)
NABEL	Switzerland	Urban or regional background	–	Barmpadimos et al. (2011)
IMPROVE	USA	Regional background	1985-	Murphy et al. (2011)
GUAN	Germany	Roadside to high Alpine	2009-	Birmili et al. (2015); Birmili et al. (2016)

[a] Most of GUAN observatories at background category are also part of ACTRIS.

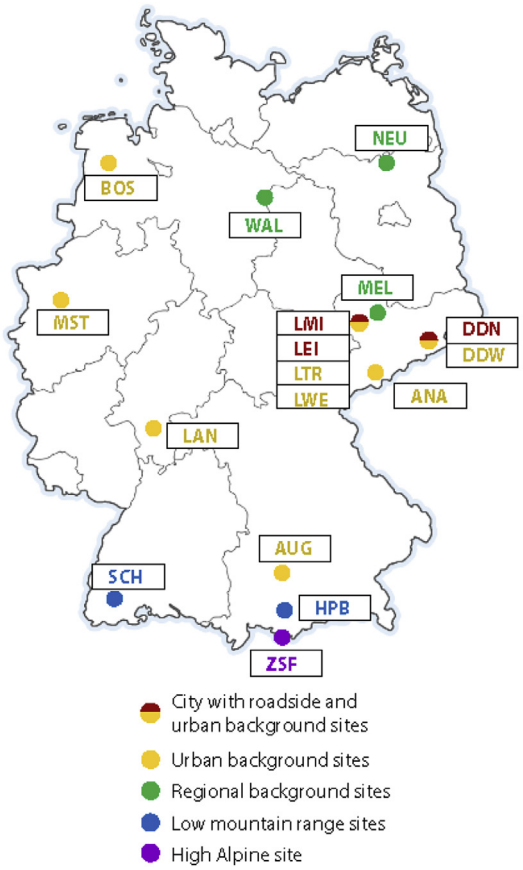

Abbreviation	Site name
ANA	Annaberg-Buchholz
AUG	Augsburg
BOS	Bösel
DDN	Dresden-Nord
DDW	Dresden-Winckelmannstraße
HPB	Hohenpeißenberg
LAN	Langen
LEI	Leipzig-Eisenbahnstraße
LMI	Leipzig-Mitte
LTR	Leipzig-TROPOS
LWE	Leipzig-West
MEL	Melpitz
MST	Mülheim-Styrum
NEU	Neuglobsow
SCH	Schauinsland
WAL	Waldhof
ZSF	Zugspitze (Schneefernerhaus)

Fig. 1. Atmospheric measurement sites in the German Ultrafine Aerosol Network (GUAN). Table on the right side illustrates the site names and abbreviations.

2. Data and methods

2.1. The German Ultrafine Aerosol Network (GUAN)

The data evaluated in this study were collected in GUAN. The measurement sites, instrumentation, data processing procedures and products are described in detail in Birmili et al. (2016). The data used in this study includes PNSD and eBC mass concentration, which have been measured continuously since 2009 at 17 atmospheric observatories in Germany. As illustrated in Fig. 1 and summarized in Table 2, the 17 observation sites allow capturing atmospheric aerosol properties in different geographic locations and environments in a large spatial scale.

GUAN includes five site categories. (1) Roadside: the sites are located nearby traffic, such as kerbside or street canyon. The distance between site and main road should is less than 10 m. (2) Urban background: the sites are located in a campus, park or residence area in city, or near a street with no or little traffic. The pollutants in urban background site are well-mixed and their concentrations are not dominantly influenced by any single source. (3) Regional background: the sites are located in areas with nature ecosystems, forests, farmland or small settlements with little or no motorway, and no industrial influence. (4) Low mountain range: the sites are located on the hill and can detect both local pollution and airmasses influence. The altitudes of the sites are between 1000 and 2000 m. (5) High Alpine: The site is located in

Table 2
Atmospheric measurement sites in GUAN, in alphabetic order (Birmili et al., 2016).

No.	Site name	Abbreviation	Status	Site category	Altitude	Location
1	Annaberg-Buchholz	ANA	In operation	Urban background	545 m	50°34'18" N, 12°59'56" E
2	Augsburg	AUG	In operation	Urban background	485 m	48°21'29" N, 10°54'25" E
3	Bösel	BOS	Terminated end of 2014	Urban background	17 m	52°59'53" N, 07°56'34" E
4	Dresden-Nord	DDN	In operation	Roadside	116 m	51°03'54" N, 13°44'29" E
5	Dresden-Winckelmannstraße	DDW	In operation	Urban background	120 m	51°02'10" N, 13°43'50" E
6	Hohenpeißenberg	HPB	In operation	Low mountain range	980 m	47°48'06" N, 11°00'34" E
7	Langen	LAN	In operation	Urban background	130 m	50°00'18" N, 08°39'05" E
8	Leipzig-Eisenbahnstraße	LEI	In operation	Roadside	120 m	51°20'45" N, 12°24'23" E
9	Leipzig-Mitte	LMI	In operation	Roadside	111 m	51°20'39" N, 12°22'38" E
10	Leipzig-TROPOS	LTR	In operation	Urban background	126 m	51°21'10" N, 12°26'03" E
11	Leipzig-West	LWE	Terminated end of 2016	Urban background	122 m	51°19'05" N, 12°17'51" E
12	Melpitz	MEL	In operation	Regional background	86 m	51°31'32" N, 12°55'40" E
13	Mülheim-Styrum	MST	In operation	Urban background	37 m	51°27'17" N, 06°51'56" E
14	Neuglobsow	NEU	In operation	Regional background	70 m	53°08'28" N, 13°01'52" E
15	Schauinsland	SCH	In operation	Low mountain range	1205 m	47°54'49" N, 07°54'29" E
16	Waldhof	WAL	In operation	Regional background	75 m	52°48'04" N, 10°45'23" E
17	Zugspitze (Schneefernerhaus)	ZSF	In operation	High Alpine	2670 m	47°25'00" N, 10°58'47" E

Table 3
Representativeness of the PNCs and eBC mass concentration in this study.

Parameter	Size interval	Particle mode	Representativeness
$N_{[10\text{-}30]}$	10–30 nm	Young Aitken mode particles	Freshly formed by nucleation from photochemistry, traffic exhausts or airport emissions (Birmili et al., 2013; Hofman et al., 2016).
$N_{[30\text{-}200]}$	30–200 nm	Aitken mode particles	Fresh emissions from incomplete combustion consist mainly of diesel soot, and aged nucleation mode particles through condensation and coagulation.
$N_{[200\text{-}800]}$	200–800 nm	Aged accumulation mode particles	The result of aging processes and long-range transport (Costabile et al., 2009).
$N_{[20\text{-}800]}$	20–800 nm	Total PNC	Tends to be dominated by UFP due to their high number fraction.
eBC	–	–	Produced by incomplete combustion of fossil fuels or biomass.

the Alpine mountain and its altitude is higher than 2000 m, meaning the airmass from free troposphere can be sampled.

There are three roadside sites in GUAN. Leipzig-Eisenbahnstraße (LEI) is located in a street canyon in the city of Leipzig. Leipzig-Mitte (LMI) and Dresden-Nord (DDN) are in an open orographic setting located in the city of Leipzig and Dresden, with 3 m and 7 m away from roadways, respectively. Traffic volumes at these sites are 12 000 vehicles per day at LEI, 44 000 vehicles per day at LMI and 36 000 vehicles per day at DDN.

Among the eight urban background sites, two are located in the city of Leipzig: Leipzig-TROPOS (LTR) and Leipzig-West (LWE). Measurements at LTR are conducted at the roof of the Leibniz Institute for Tropospheric Research (TROPOS) main building; while LWE is located in a hospital park area in the west of Leipzig. Dresden-Winckelmannstraße (DDW) and Annaberg-Buchholz (ANA) are also located in the State of Saxony. DDW is located in the city of Dresden, about 1.7 km south from the city center. ANA is located in the city of Annaberg-Buchholz in the Ore Mountains (Erzgebirge), a mountain range in SE Germany. Three urban background sites are located in the western part of Germany: Langen (LAN), Mülheim-Styrum (MST) and Bösel (BOS). LAN is located in the city of Langen, at the edge of a residential area and a forest. It is about 10 km south of the city of Frankfurt am Main and 5 km southeast of Frankfurt's Rhein-Main airport. Depending on the wind direction, emissions from the airport may sometimes influence the measurement. The site MST is situated within a residential area in the western end of the Ruhr area, the largest urban agglomeration in Germany, and it qualifies as an urban background monitoring site (Quass et al., 2004). The land-use regression modelling and chemistry transport modelling results showed that, MST is driven more by industrial sources than other urban background sites (Hennig et al., 2016). BOS is an urban background site near the village of Bösel. The site is 100 km from the North Sea, so clean maritime air masses can reach there. The site AUG is located on the premises of Augsburg's University of Applied Sciences and is the only urban background site in the southern Germany in GUAN.

Three regional background sites are located in the North German lowland: Neuglobsow (NEU), Melpitz (MEL) and Waldhof (WAL). Since they are distant from major highways and population centers (population greater than ca. 500 000), NEU and WAL represent the regional background conditions in the North German lowlands. MEL is located in a rural setting in Eastern Germany surrounded by pasture, forests, and little villages, and can be considered as a regional background site of central Europe (Engler et al., 2007; Spindler et al., 2013).

Three mountain sites are located at the southern Germany. Two low mountain range sites Schauinsland (SCH, 1205 m a.s.l.) and Hohenpeißenberg (HPB, 980 m a.s.l.) are surrounded mainly by forests and agricultural lands. The High Alpine site Zugspitze (ZSF, Schneefernerhaus) is located at 2670 m a.s.l., near the summit of the mountain Zugspitze – Germany's highest mountain.

2.2. Instrumentation

Atmospheric aerosol measurements in this study include PNSD and eBC mass concentrations. Details of the instrumentation and data processing are available in Birmili et al. (2016). Only a short summary is given in this section and Appendix Table S1. Aerosol PNSD is measured by Mobility Particle Size Spectrometers (MPSS, Wiedensohler et al., 2012). Depending on their individual set-up, these instruments are called MPSS, Tandem Mobility Particle Size Spectrometers (TMPSS) and Thermodenuder Mobility Particle Size Spectrometers (TDMPSS). The use of Nafion dryers ensures a relative humidity of the sampled aerosol below 40%. Therefore, aerosol particles are sized at a relatively dry, i.e., dehydrated state. The PNSD was obtained from the raw mobility distributions by a multiple charge inversion (Pfeifer et al., 2014). The corrections for internal and sampling losses due to diffusion and sedimentation were corrected as described in Wiedensohler et al. (2012).

Due to the different settings of MPSS at GUAN sites, the MPSS data quality at each site was assured by on-site or laboratory inter-comparisons with reference instruments conducted by the World Calibration Center for Aerosol Physics (WCCAP) at TROPOS, Leipzig, Germany, following the recommendations given in Wiedensohler et al. (2017). It is essential to define a standard for inter-comparisons with reference instruments. In GUAN, a condensation particle counter (CPC, model 3010/3772, TSI Inc., Schoreview, USA) and an electrometer (model 3068B, TSI Inc., Schoreview, USA) were used as an intermediate standard for PNC (Birmili et al., 2016). These inter-comparisons were done in the central laboratory, at calibration workshops, or in the field as part of a “round-robin test”. The frequency of the inter-comparisons was site-dependent varying between once to four times per year.

To condense the information provided by the PNSD, we calculated PNCs with three particle size intervals, as shown in Table 3. $N_{[10\text{-}30]}$ represents particles freshly formed from nucleation, either by photochemical processes or downstream of traffic exhausts or airport emissions. Particles emitted from incomplete combustion can be found mainly in size range 30–200 nm, and can be well represented by $N_{[30\text{-}200]}$. $N_{[200\text{-}800]}$ is more representative for aged particles and the influence of long-range transport. Since the PNSD were measured only for particle diameter greater than 20 nm at MST, to maintain the consistence of total PNC among different sites, we use $N_{[20\text{-}800]}$ to evaluate the total PNC.

eBC mass concentrations were measured with Multi-Angle Absorption Photometers (MAAP, model 5012, Thermo Scientific), except in AUG where an aethalometer (Type 8100, Thermo Fisher Scientific Inc.) was used. eBC mass concentration was calculated using a mass absorption cross section of 6.6 $m^2\,g^{-1}$ at wavelength $\lambda = 637$ nm. The use of an constant mass absorption cross section may introduce an uncertainty in eBC mass concentration, especially for aged BC particles. There was no eBC data available at LAN and MST.

Data coverage over the period from 2009 to 2014 is shown in Table 4. PNSD and eBC have been measured since 2009 except six sites: three sites (LMI, LWE, and LAN) started their measurements in 2010, one (NEU) started in 2011, and the other two (ANA and DDW) started in 2012. It can be seen from Table 4, most of the sites have at least data for three or four years with more than 75% annual data coverage. In general, the overall data coverage is adequate for detecting the main

Table 4
Data coverage of particle number concentration and eBC.

Sites	Data coverage of eBC (%)							Data coverage of PNSD (%)						
	Total	2009	2010	2011	2012	2013	2014	Total	2009	2010	2011	2012	2013	2014
DDN	89	95	99	95	56	93	97	73	56	70	89	50	85	87
LEI	92	96	95	99	100	81	82	82	33	99	88	98	88	85
LMI	71	–[a]	50	94	95	99	91	67	–[a]	40	90	89	93	93
MST	No data							86	76	76	89	79	95	100
LTR	97	100	97	95	93	100	99	94	97	96	84	94	93	96
LWE	68	–[a]	48	97	97	92	78	69	–[a]	48	82	99	98	84
ANA	44	–[a]	–[a]	–[a]	85	96	85	43	–[a]	–[a]	–[a]	84	84	87
AUG	81	96	99	99	99	95	–[b]	80	92	99	99	96	93	–[b]
DDW	44	–[a]	–[a]	–[a]	75	95	94	36	–[a]	–[a]	–[a]	63	89	63
LAN	No data							48	–[a]	16	79	99	76	17
BOS	85	92	98	86	71	79	81	89	87	99	86	76	100	83
MEL	98	100	100	100	100	100	91	90	90	87	78	97	94	95
WAL	71	24	99	99	77	98	31	95	97	91	93	91	98	97
NEU	78	–[a]	85	96	90	98	98	51	–[a]	–[a]	59	52	98	99
HPB	100	100	100	100	100	100	99	93	97	99	81	90	93	97
SCH	82	95	83	79	49	85	99	84	91	98	74	67	84	89
ZSF	89	99	100	69	84	94	90	74	96	80	68	67	94	40

[a] PNSD or eBC was not measured.
[b] Data in 2014 at site AUG was not provided for this study.

characteristics of the parameters. In this study, a data coverage threshold of 75% was used in the calculation of diurnal and annual cycles.

2.3. Clustering methods

To better understand the spatial variability of aerosol particles, a clustering analysis was applied in this study. Clustering analysis provides a way to identify the common characteristics of observations by the behaviors of the data itself. Usually it tends to group observation data into subsets that similar observations are grouped together, while different observations belong to different groups (Rocach and Maimon, 2005).

The clustering method used in this study is an agglomerative hierarchical clustering. Each observation initially represents a cluster of its own. Then clusters are gradually merged until the whole cluster structure is generated. A dendrogram shows the similarity distance at different cluster levels. Then the final clustering result can be obtained by cutting the dendrogram with a predefined similarity threshold (Rocach and Maimon, 2005).

Firstly, the similarity distance of the time series between each pair of sites was calculated. Commonly used metrics include distance metrics (Euclidean distance, Manhattan distance etc.) and similarity metrics (Pearson correlation coefficient etc.). Since the aerosol parameters analyzed here may not be normally distributed, it is more appropriate to use the Spearman's rank correlation coefficient to determine the distance $D_{x,y}$:

$$D_{x,y} = 1 - r_{x,y} \quad (1)$$

where $r_{x,y}$ is the Spearman's rank correlation coefficient between the time series x_i and y_i at two sites. It will be high when the data points x_i and y_i have a similar rank and low when data points x_i and y_i have a dissimilar rank (Kruskal, 1958). Thus $D_{x,y}$ can identify whether two observations are concurrently increasing or decreasing. In detail, for two time series x_i and y_i with the same size, they are firstly converted to ranks rgx_i and rgy_i. Then $r_{x,y}$ is determined by:

$$r_{x,y} = \frac{cov(rgx,\ rgy)}{\sigma_{rgx}\sigma_{rgy}} \quad (2)$$

where cov(rg*x*,rg*y*) is the covariance of the rank variables; σ_{rgx} and σ_{rgy} are the standard deviation of the rank variables (Myers et al., 2010).

As the similarity distance is determined, a linkage criterion can be used to define whether two clusters should be grouped together. There are several commonly used linkage criteria, e.g., single, complete, and average linkages. In our study, a complete linkage clustering criterion was used. The distance between two clusters was obtained as the longest distance from any member of one cluster to any member of the other cluster (King, 1967). Usually the complete linkage can provide more compact clusters and more useful hierarchies (Rocach and Maimon, 2005).

Finally, a dendrogram can be generated. Each level of the hierarchy represents a particular grouping of data into disjoint clusters. The entire hierarchy represents an ordered sequence of such groupings (Hastie et al., 2009). Usually, a predefined similarity threshold can be used to determine the clusters.

3. Overview of the dataset

3.1. Basic statistics

Currently used site categories, such as roadside, urban background, regional background etc. clearly denotes the influence of anthropogenic sources which is one of the main factors determining the pollutant concentrations. Basic statistics of PNCs, PNSD and eBC mass concentration for different site categories are analyzed in this section.

Table 5 illustrates the multi-annual statistics of eBC mass concentration and PNC for different size intervals at all GUAN sites. μ_{50}, std, μ_{25} and μ_{75} denote the median, standard deviation, 25th and 75th percentile values, respectively. At a first glance, remarkable differences can be seen in the overall median values between site categories, but the difference between the sites in the same category is relatively small. The median values of $N_{[20\text{-}800]}$ range from 900 cm^{-3} at the High Alpine site ZSF to 9000 cm^{-3} at the roadside site LMI; and eBC mass concentrations range from 0.1 to 2.3 $\mu g/m^3$. PNCs and eBC mass concentration decrease from roadside to urban background, followed by regional background, low mountain range and High Alpine. Due to the industrial influence from Ruhr area (Beuck et al., 2011), the PNC below 200 nm at MST are quite close to those at the three roadside sites.

Fig. 2 illustrates the median PNSDs at the five site categories. Significant difference can be seen among the five median PNSDs. Contributed by traffic emissions, PNSD at roadside sites shows a prominent peak at about 20 nm. And the peak moves to 40 nm at urban background sites. At regional background and low mountain range sites, the peaks move further to about 60 nm. It is interesting to note that the

Table 5
Statistics of eBC mass concentration and PNCs at all 17 GUAN sites, based on hourly values. μ_{50}, std, μ_{25} and μ_{75} denote the median, standard deviation, 25th and 75th percentile values, respectively.

Site category	Site name	eBC (μg/m[c])				$N_{[20\text{-}800]}$ (cm^{-3})				$N_{[10\text{-}30]}$ (cm^{-3})				$N_{[30\text{-}200]}$ (cm^{-3})				$N_{[200\text{-}800]}$ (cm^{-3})			
		μ_{50}	std	μ_{25}	μ_{75}	μ_{50}	std	μ_{25}	μ_{75}	μ_{50}	std	μ_{25}	μ_{75}	μ_{50}	std	μ_{25}	μ_{75}	μ_{50}	std	μ_{25}	μ_{75}
Roadside	DDN	**2.1**	1.6	1.3	3.2	**8380**	5486	5822	11893	**4647**	4810	2630	7787	**5872**	3962	4079	8320	**533**	422	342	791
	LEI	**1.7**	1.7	1.0	2.8	**8458**	5598	5818	11950	**5394**	6294	3346	8761	**6019**	4083	4080	8509	**454**	449	279	722
	LMI	**2.3**	2.0	1.4	3.6	**9012**	6450	6111	13077	**4938**	5578	2956	8256	**6367**	4505	4254	9146	**517**	419	328	785
	Mean value	**2.0**	–	–	–	**8617**	–	–	–	**4993**	–	–	–	**6086**	–	–	–	**501**	–	–	–
Urban background	MST	– [b]	– [b]	– [b]	– [b]	**7421**	4883	5136	10712	– [b]	– [b]	– [b]	– [b]	**5184**	3809	3454	7702	**368**	335	217	572
	LTR	**0.8**	1.3	0.5	1.5	**4840**	4110	3229	7216	**2351**	5067	1371	4013	**3369**	2903	2215	5141	**354**	344	202	573
	LWE	**0.8**	1.2	0.5	1.5	**4381**	3297	2945	6486	**1999**	4011	1263	3166	**3059**	2419	2007	4653	**320**	332	181	528
	ANA	**1.1**	1.8	0.6	2.0	**4318**	5608	2710	6988	**2168**	5178	1052	4369	**3563**	4819	2216	5821	**396**	429	235	633
	AUG	**1.4**	1.5	1.0	2.2	**5644**	5764	3716	9045	**2659**	6551	1613	4424	**3871**	4313	2522.4	6309	**289**	304	158	466
	DDW	**0.9**	1.1	0.4	1.6	**4600**	3921	3029	6862	**2128**	3621	1287	3541	**3827**	3506	2446	5839	**394**	329	221	643
	LAN	– [c]	– [c]	– [c]	– [c]	**5722**	3830	3757	8386	**4088**	5219	2532	6569	**3985**	2835	2568	6028	– [c]	– [c]	– [c]	– [c]
	BOS	**0.5**	0.8	0.3	1.0	**4812**	3123	3226	6838	**1647**	2184	1050	2578	**3490**	2474	2252	5122	**376**	337	202	602
	Mean value[a]	**0.9**	–	–	–	**4902**	–	–	–	**2434**	–	–	–	**3595**	–	–	–	**352**	–	–	–
Regional background	MEL	**0.5**	1.2	0.3	1.1	**3714**	2998	2538	5322	**1009**	3199	570	1768	**2668**	2205	1764	3952	**337**	346	190	546
	WAL	**0.4**	0.7	0.2	0.8	**3391**	2350	2240	4892	**871**	1876	474	1515	**2443**	1888	1551	3687	**316**	325	169	524
	NEU	**0.4**	0.9	0.2	0.8	**2936**	1844	2036	4085	**416**	1411	200	817	**2218**	1477	1462	3170	**279**	291	157	476
	Mean value	**0.4**	–	–	–	**3347**	–	–	–	**765**	–	–	–	**2443**	–	–	–	**311**	–	–	–
Low mountain range	HPB	**0.3**	0.4	0.2	0.5	**2360**	1468	1550	3377	**588**	829	333	973	**1737**	1139	1131	2532	**223**	242	97	397
	SCH	**0.2**	0.4	0.1	0.4	**1641**	1429	902	2635	**360**	832	180	719	**1207**	1086	664	1977	**148**	190	58	296
	Mean value	**0.3**	–	–	–	**2000**	–	–	–	**474**	–	–	–	**1472**	–	–	–	**185**	–	–	–
High Alpine	ZSF	**0.1**	0.2	0.0	0.2	**886**	874	469	1562	**183**	543	96	357	**708**	744	381	1226	**69**	164	19	205

[a] Site MST is not included in means.
[b] Parameter is not measured.
[c] Parameters are not included at LAN due to quality assurance.

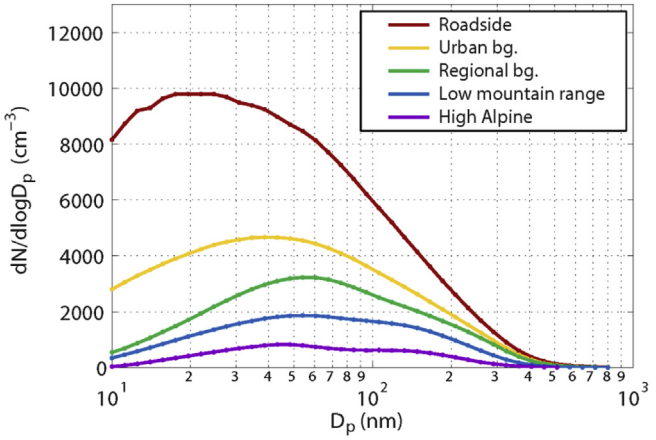

Fig. 2. Median PNSDs for the five site categories.

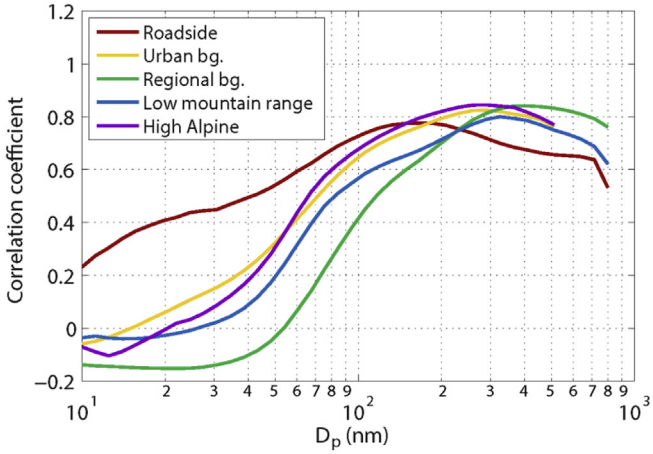

Fig. 3. Cross-correlation between PNSD and eBC mass concentration at each site category.

peak of the PNSD moves towards larger diameters with the increasing distance between the sites and emission sources, reflecting the aging of aerosol particles during its transport from sources to remote area. During these processes, aerosol particles may grow due to condensation and coagulation (Van Dingenen et al., 2004), resulting in the change of the shape of PNSD as shown in Fig. 2.

3.2. Cross-correlation of measured parameters

The average PNCs are elevated at urban sites mainly due to anthropogenic emissions, but other sources such as new particle formation (NPF) may also contribute to the PNCs (Reche et al., 2011). Since eBC is a more robust tracer of traffic emission and other non-traffic combustion sources such as power plants and domestic heating (Chen et al., 2014; Di Ianni et al., 2018; Hitzenberger and Tohno, 2001; Pérez et al., 2010), the cross-correlation between PNSD and eBC mass concentration was analyzed to detect the influence of anthropogenic sources at different site categories. Fig. 3 shows the Pearson's correlation coefficient between PNSD and eBC mass concentration.

Higher correlation coefficient can be observed at roadside compared to the other four site categories in ultrafine size range ($D_p < 100$ nm), confirming a stronger traffic influence. Moreover, two modes can be found in the size-resolved correlation coefficient at roadside category: one at 20–30 nm and the other at 100–200 nm, respectively indicating the emission of gasoline engines and diesel engines (Harris and Maricq, 2001). The correlation coefficient curves show similar shapes at the other four site categories. No correlation (correlation coefficients range from −0.2 to 0.2) can be seen in the size range of 10–30 nm. The correlation coefficient increases with increasing particle size, and finally reaches its maximum when particle diameter is larger than 200 nm. Since young Aitken mode particles may grow very fast into Aitken mode, fresh traffic-emitted particles can be hardly observed in this mode in these four site categories. The observed Aitken mode particles are mainly originated from NPF. Therefore, there is nearly no correlation between eBC mass concentration and Aitken mode PNC. At the sites in these four categories, the observed eBC is mostly aged, and

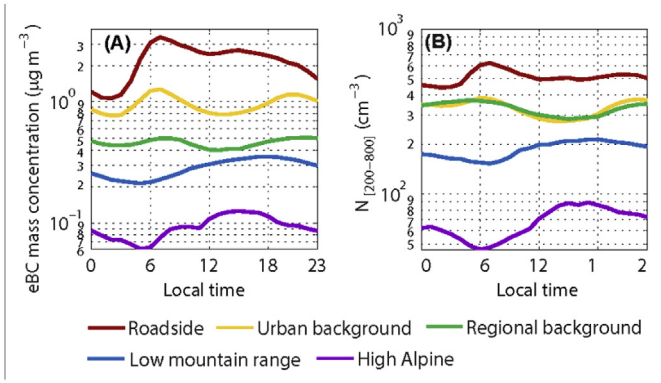

Fig. 4. Diurnal cycles of eBC mass concentration **(A)** and $N_{[200\text{-}800]}$ **(B)** on weekday (Monday to Friday) for different site categories.

locates in a size range larger than 100 nm. Higher correlation coefficients are thus yielded between eBC mass concentration and PNC at diameter larger than 100 nm.

3.3. Diurnal cycles of aged accumulation mode particle number and equivalent black carbon mass concentrations

Fig. 4 illustrates the diurnal cycles of eBC mass concentration and aged accumulation mode particle number concentration $N_{[200\text{-}800]}$ on weekdays (Monday to Friday) for different site categories. More detailed diurnal and annual cycles of all parameters on weekday, Saturday and Sunday can be found in Appendix Fig. S2 and S3.

Since eBC is a source driven parameter dominated mainly by anthropogenic emissions especially by traffic, significant differences in diurnal cycles of eBC mass concentration were observed among the five site categories, as seen in Fig. 4(A). The diurnal pattern of eBC mass concentration for different site categories will be discussed in more detail in Sect. 4.2. PNC is a non-conserved quantity and determined by many size-dependent processes. The diurnal cycles of PNC thus show different patterns with respect to their size ranges, as shown in Fig. S2. In Fig. 4(B), the diurnal patterns of $N_{[200\text{-}800]}$ at urban background and regional background sites are very similar. It means, to a certain extent, "site category" is not always a valid way to catch the spatial variability of accumulation mode particles which is mainly determined by aging and long-range transport. "Site category" provides the information about the influence of anthropogenic sources. Parameters controlled by other processes might be identical between different site categories.

In general, for "source driven" pollutant parameters such as eBC mass concentration, their spatial variability is highly connected to the categories of the measurement sites. Conversely, for pollutant parameters which are more influenced by other factors such as aging processes and meteorological conditions, we may need other ways to evaluate their spatial variabilities. There are several other parameters to characterize a site, e.g. locations, elevations, topographies and meteorological conditions. By extracting "site groups" according to certain characteristics, it might be possible to investigate how pollutant parameters interfere with spatial characteristics.

4. Spatial clustering analysis

4.1. Size-dependent similarity distance of particle number size distribution between sites

In this section, the size-dependent spatial characteristic of particle number concentrations was investigated with Spearman's correlation distance. As described in Sect. 2.3, Spearman's correlation distance $D_{x,y}$ can be used to determine the similarity between a pair of time series. Usually, Spearman's correlation distance $D_{x,y}$ could be interpreted as following:

- $D_{x,y} = 2$ ($r_{x,y} = -1$): perfect negative correlation;
- $1.8 \leq D_{x,y} < 2$ ($-1 < r_{x,y} \leq -0.8$): strong negative correlation;
- $1.4 \leq D_{x,y} < 1.8$ ($-0.8 < r_{x,y} \leq -0.4$): moderate negative correlation;
- $1 < D_{x,y} < 1.4$ ($-0.4 < r_{x,y} < 0$): weak negative correlation;
- $D_{x,y} = 1$ ($r_{x,y} = 0$): no correlation;
- $0.6 < D_{x,y} < 1$ ($0 < r_{x,y} < 0.4$): weak positive correlation;
- $0.2 < D_{x,y} \leq 0.6$ ($0.4 \leq r_{x,y} < 0.8$): moderate positive correlation;
- $0 < D_{x,y} \leq 0.2$ ($0.8 \leq r_{x,y} < 1$): strong positive correlation;
- $D_{x,y} = 0$ ($r_{x,y} = 1$): perfect positive correlation.

To characterize the spatial variability of particle number concentration at different sizes, the similarity distance of PNSDs between site pairs within the same site category (urban background and regional background) is calculated as shown in Fig. 5. Although with different absolute levels, the size-resolved $D_{x,y}$ for different site pairs show very similar patterns, with higher values in size range of 10–30 nm and lower values in 100–800 nm. This result clearly illustrates the spatial variability of aerosol particles with different sizes. Particles in 10–30 nm are dominated by various local sources and NPF, and may grow rapidly to larger sizes via coagulation and condensation, leading to a higher spatial variability. In contrast, particles in accumulation mode have a longer lifetime and tend to distribute homogeneously in the background air in a relatively large area, therefore show a lower

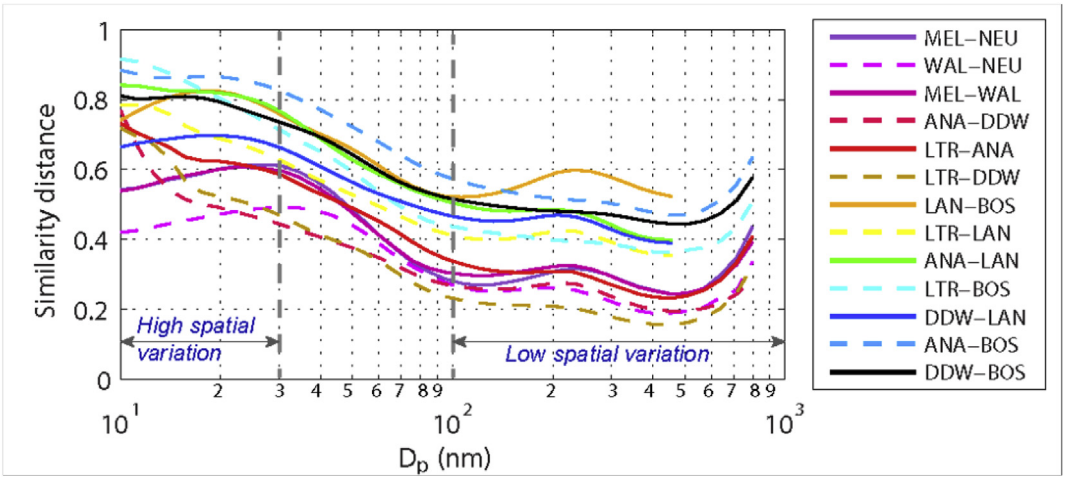

Fig. 5. Similarity distance of particle number size distributions between site pairs within the same category (urban and regional background).

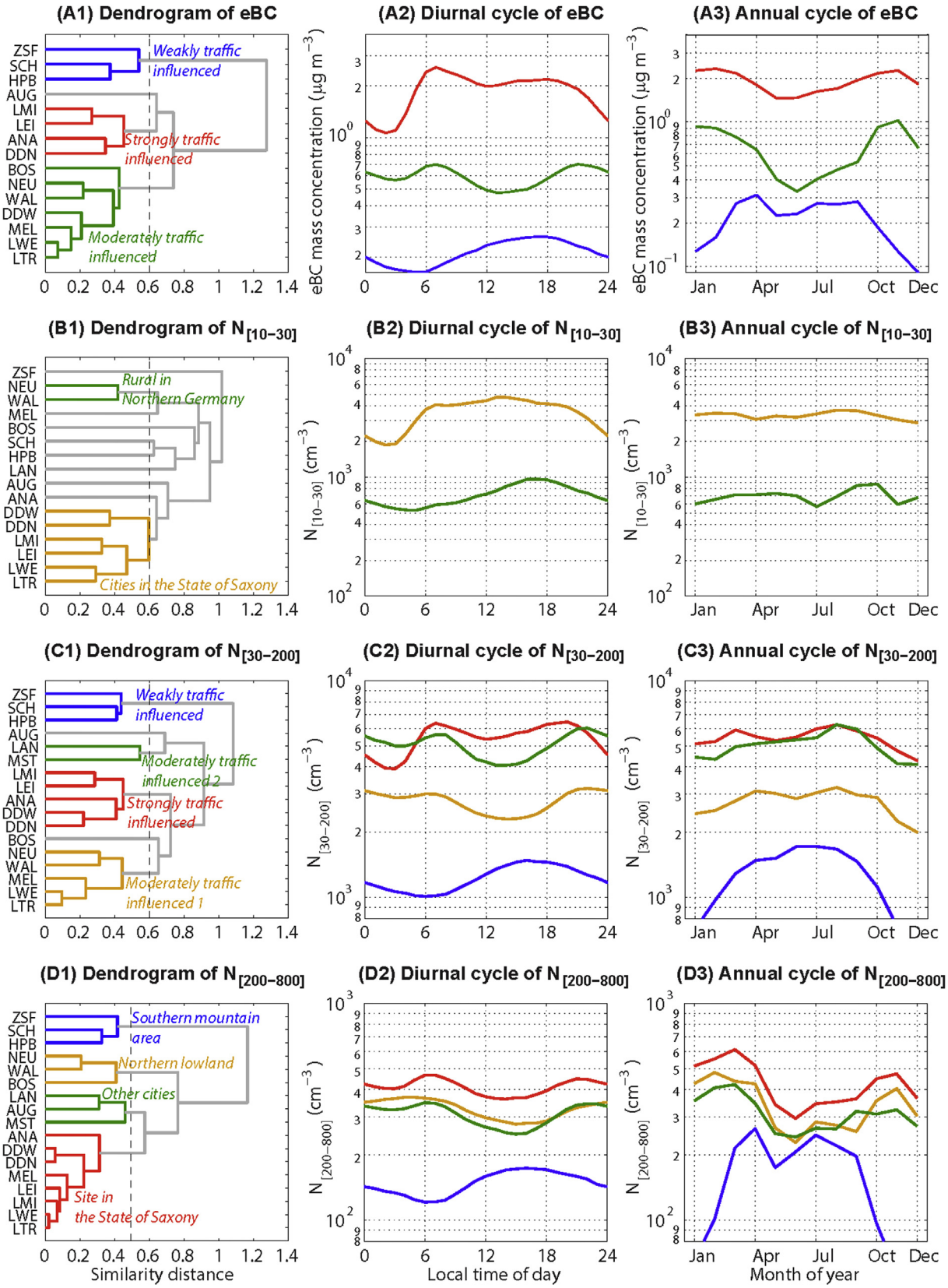

Fig. 6. Hierarchical clustering results of PNC and eBC mass concentration based on hourly time series (left column) and the diurnal and annual cycles of pollutant parameters for each group (middle and right column).

spatial variability. It can be seen that $D_{x,y}$ increases again for particle diameter larger than 600 nm. A plausible explanation is that this size range is in the tail of coarse mode in which particles have relative short lifetime due to gravity settling.

Accordingly, three size intervals are extracted regarding to the similarity distance curve: a higher spatial variability size range 10–30 nm, a transition size range 30–100 nm and a lower spatial variability size range 100–800 nm. Since the particles in 30–200 nm contains most of eBC mass in urban area (Cheng et al., 2013), to better catch the variability of eBC, we will use $N_{[30\text{-}200]}$ and $N_{[200\text{-}800]}$ instead of $N_{[30\text{-}100]}$ and $N_{[100\text{-}800]}$ to evaluate the behavior of particles in transition size range and lower spatial variability size range.

4.2. Hierarchical clustering of particle number and eBC mass concentrations

Based on the similarity distance, a dendrogram was generated following the hierarchical clustering methodology described in Sect. 2.3 and the sites were classified with a predefined threshold D_0. In this study, we used a threshold $D_0 = 0.6$ to extract clusters, meaning that the observations in the same group are at least moderately positive correlated. The clustering was based on hourly time series. Fig. 6 illustrates the clustering results and the corresponding diurnal and annual cycles for each group. For a certain pollutant parameter, the measurements at sites in the same group have similar temporal variation, indicating a high spatial homogeneity of the parameter among these sites. Conversely, the sites in different groups represent high spatial variability of the parameter. In this section, we name each group in the dendrogram according to the common characteristic of the sites in the group.

4.2.1. Equivalent black carbon mass concentration

Fig. 6(A1) shows the clustering result of the eBC mass concentration. Since the eBC mass concentration is a typical tracer for anthropogenic emissions, especially traffic emissions, Fig. 6(A1) shows the degree of traffic influence at the sites. Three groups, namely *"Weakly traffic influenced"*, *"Strongly traffic influenced"* and *"Moderately traffic influenced"*, are distinguished under a threshold of 0.6.

Strongly traffic influenced group includes all three roadside sites (LMI, LEI and DDN), and one urban background sites ANA. ANA is located very close to the national road B101 with a distance of 10 m, therefore it can be considered as a strongly traffic influenced urban background site. AUG cannot be classified into any cluster under a threshold 0.6, but can be grouped into the *Strongly traffic influenced* cluster under a threshold 0.65, meaning that AUG can be defined as a traffic influenced urban background site, which is consistent with a previous study (Cyrys et al., 2008). As shown in Fig. 6(A2), in the *Strongly traffic influenced* group, the eBC mass concentration stays at a lower level after midnight (00:00 LT - 04:00 LT), then rapidly increases after 04:00 LT and reaches its first peak at 07:00 LT resulting from the morning traffic and near ground temperature inversion (Olofson et al., 2009; Birmili et al., 2013; Wehner et al., 2002). The second peak occurs around 15:00 LT during the afternoon rush hour. In general, the diurnal pattern of eBC mass concentration in the *strongly traffic influenced* group is mainly determined by traffic emission and the evolution of boundary layer. The annual cycle of eBC mass concentration shows higher concentration levels in the cold season than in the warm season. During the cold season, more BC is emitted from domestic heating and power plants. Moreover, lower plenary boundary layer (PBL) in the cold season inhibits the vertical dispersion of BC and thus elevates the eBC mass concentration in the boundary layer.

The sites in *weakly traffic influenced* group include low mountain range and high Alpine sites which are barely influenced by anthropogenic emissions. Blue curves in Fig. 6(A2) and (A3) show the corresponding diurnal and annual cycles. The diurnal and annual cycles of this group show opposite behaviors from those of other groups, because aerosol concentrations are mainly determined by PBL due to the high elevation of these sites (Birmili et al., 2010; Collaud Coen et al., 2014; Lugauer et al., 1998, 2000). Mountain sites, especially ZSF, stay regularly in clean air in the free troposphere in cold season from October to March. Conversely, during the warm season, polluted aerosol can be transported to the mountain sites since the sites are mainly inside the developed boundary layer. For diurnal cycle, resulting from the diurnal evolution of PBL, eBC mass concentration stays at a low level in the early morning (03:00 LT – 07:00 LT), then increases around noon as the boundary layer air reaches the site.

The third group *moderately traffic influenced* includes all the other urban and regional background sites. These sites are split into three sub-groups: urban sites (LTR, LWE, MEL and DDW), regional sites (NEU and WAL) and BOS. BOS is located in a rural setting, but is strongly influenced by a residential area in the village Bösel. BOS is thus a site in between of urban background and regional background. The regional background site MEL is grouped together with three urban background sites (DDW, LWE and LTR), because these four sites are located very close to each other. All these sites are usually influenced by the same plumes of BC originated from domestic heating in Eastern Europe. The diurnal cycle of the *moderately traffic influenced* group shows different behaviors compared to the previous two clusters. Due to the inhibited boundary layer coupled with increased anthropogenic emission such as traffic, cooking and heating, two peaks can be observed respectively in the morning (06:00 LT – 08:00 LT) and evening (around 20:00 LT and 21:00 LT). Far from traffic sources, evolution of boundary layer seems to play a more pronounced role in the diurnal cycle of eBC mass concentration. Therefore, no peak can be observed at rush hour in the afternoon (15:00 LT). The annual cycle of this group shows a similar pattern but at a lower concentration level compared with the one in the *Strongly traffic influenced* cluster due to their farther distance from traffic sources.

From the clustering result and corresponding temporal variation of eBC mass concentration, it can be concluded that the spatial distribution of eBC mass concentration in Germany is mainly determined by the distribution of anthropogenic emission sources, especially traffic sources. The evolution of boundary layer is also a major factor determining the mass concentration of eBC especially at urban background and mountain sites.

4.2.2. Young Aitken mode particles $N_{[10\text{-}30]}$

As discussed in Sect. 4.1, PNC in the size range of 10–30 nm shows the highest spatial variability among the parameters studied. Only two groups are extracted under a threshold of 0.6: "*Rural in Northern Germany*" and "*Cities in the State of Saxony*".

Rural in Northern Germany group includes WAL and NEU, which are relatively far from urban areas or anthropogenic emissions. In the diurnal cycle of this group, $N_{[10\text{-}30]}$ increases from 11:00 LT to the late afternoon, mainly relating to the NPF (Zíková and Ždímal, 2013). Only minor annual variation can be seen in the annual cycle of $N_{[10\text{-}30]}$. The reason might be that high $N_{[10\text{-}30]}$ only appears in very short time periods since the newly formed particles grow rapidly up to 50–100 nm during an NPF event (Kulmala et al., 2001). Therefore, the use of median values may mask the influence of high concentrations which are only shortly occurred during NPF events in the annual cycle.

Sites LTR, LWE, LEI, LMI, DDN and DDW are grouped into *Cities in the State of Saxony* cluster. In these urban sites, both NPF and traffic emission have impacts on the diurnal variation of $N_{[10\text{-}30]}$. The first peak in its diurnal cycle is observed at 06:00 LT due to traffic emission, then another small peak can be seen around noon relating to NPF events in the area (Birmili et al., 2013; Ma and Birmili, 2015).

$N_{[10\text{-}30]}$ has the highest spatial variability among the parameters studied due to the short lifetime of young Aitken mode particles. And it is influenced by both NPF and traffic emission. Therefore, only the sites with similar source influence and in a relatively small spatial scale are classified in the same group. Most of the sites are weakly/non-correlated and cannot be grouped as shown in Fig. 6(B1).

4.2.3. Aitken mode particles $N_{[30\text{-}200]}$

$N_{[30\text{-}200]}$ represents the particles originated from anthropogenic emissions and the aged particles originated from NPF. Clustering result of $N_{[30\text{-}200]}$ is similar as that of eBC. As shown in Fig. 6(C1), four clusters can be extracted from the hierarchy, namely *"Weakly traffic influenced"*, *"Strongly traffic influenced"*, *"Moderately traffic influenced 1"* and *"Moderately traffic influenced 2"*.

Same as the eBC clustering result, ZSF, SCH and HPB are grouped together as the *weakly traffic influenced* group. As shown in Fig. 6(C2) and (C3), the diurnal and annual cycle of $N_{[30\text{-}200]}$ in this cluster shows similar behavior as the corresponding group of eBC mass concentration (see Fig. 6(C2) and (C3)), which is dominated by the evolution of PBL, as explained in Sect. 4.2.1.

Five urban sites, LMI, LEI, ANA, DDW and DDN, are grouped into the *strongly traffic influenced* group. The diurnal cycle of the $N_{[30\text{-}200]}$ shows the same pattern as that of eBC mass concentration, indicating that $N_{[30\text{-}200]}$ is strongly influenced by traffic emission in urban area. But the annual cycle in this group shows a different pattern compared with eBC mass concentration. The $N_{[30\text{-}200]}$ is elevated in the warm season, contributed mainly by NPF.

Two *moderately traffic influenced* groups are extracted. The sites in the cluster *moderately traffic influenced 1* (NEU, WAL, MEL, LWE and LTR) are mainly located in the NE Germany and the sites in the cluster *moderately traffic influenced 2* (MST and LAN) are located in western Germany. The diurnal and annual cycles of these two groups show the same patterns but at different levels. The concentration level of $N_{[30\text{-}200]}$ in the *moderately traffic influenced 1* is lower than *moderately traffic influenced 2*, indicating a lower traffic emission in the sites in *moderately traffic influenced 1* group.

The clustering result of $N_{[30\text{-}200]}$ indicates that the spatial distribution of $N_{[30\text{-}200]}$ in Germany is mainly determined by the distribution of anthropogenic emission sources, especially traffic sources. But it should be noted that the clustering result also show some geographical characteristics (*Moderately traffic influenced 1* and *2*). As shown in Fig. 5, 30–100 nm is the transition size range from low spatial correlation to high spatial correlation.

4.2.4. Aged accumulation mode particles $N_{[200\text{-}800]}$

$N_{[200\text{-}800]}$ represents the well-aged accumulation mode particles. Resulting from their longer lifetime, these particles tend to distribute homogeneously in the background air in a large area. Therefore, a lower similarity distance of $N_{[200\text{-}800]}$, meaning a stronger positive correlation, can be observed between the observations at different sites. To have a more specific clustering result, a lower threshold of 0.5 is used here and the clustering result is illustrated in Fig. 6(D1). Four groups are identified and are also marked in the map in Fig. 7. We can clearly see that the sites are classified according to its geographic locations. Previous study from Bigi and Ghermandi (2014) found similar results for PM_{10} mass concentration in Po Valley in Italy, since PM_{10} mass concentration is also a parameter representing the background pollution in a large spatial scale. From this result we can conclude that the distribution of sources has only minor influence on the spatial distribution of $N_{[200\text{-}800]}$.

To sum up, a hierarchical clustering method was applied in this study to investigate how pollutant parameters interfere with spatial characteristics. In general, different parameters are controlled by different factors and thus show different spatial variabilities. The concentration of young Atiken mode particles $N_{[10\text{-}30]}$ is a "local source driven" parameter due to its short lifetime, thus show a high spatial inhomogeneity. The eBC mass concentration and $N_{[30\text{-}200]}$ are mainly determined by anthropogenic emissions, thus the sites with similar emission influence are grouped together. And the clustering result of $N_{[30\text{-}200]}$ also shows some geographical characteristics. As particles are growing larger, more "regional" and "background" characteristics are reflected in the clustering. $N_{[200\text{-}800]}$ show a high spatial homogeneity. The distribution of sources has only minor influence on its spatial distribution.

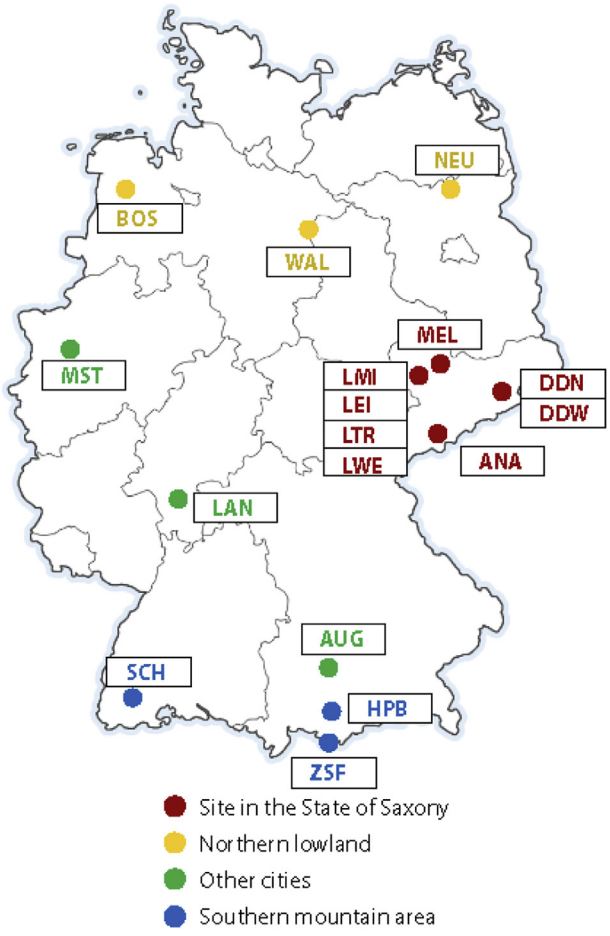

Fig. 7. Hierarchical clustering result of $N_{[200\text{-}800]}$.

4.3. Correlation between pollutant parameter similarity and geographical distance

To further investigate the spatial homogeneity of PNCs and eBC mass concentrations, the correlation between the similarity of measured parameters in site pairs and their geographical distance was analyzed in this section. Site pairs in the same category (urban, regional background or low mountain range) was selected for the calculation. Then the Pearson's correlation coefficient of the two time series was calculated and plotted versus the geographical distance between two sites as shown in Fig. 8. The three roadside sites are excluded because these sites are strongly influenced by local traffic emissions.

In general, for all parameters, the correlation coefficient decreases with increasing geographical distance, which follows the "First Law of Geography" that everything is related to everything else, but near things are more related than distant things (Tobler, 1970). However, different parameters show different sensitivities on geographical distance. As shown in Fig. 8, the overall correlation coefficients of $N_{[200\text{-}800]}$ are highest among the parameters studied and also well correlated with geographical distance. Therefore, $N_{[200\text{-}800]}$ is a good parameter to examine the spatial homogeneity of regional background aerosol. $N_{[10\text{-}30]}$ shows the lowest correlation coefficient due to the short lifetime of Young Aitken mode particles. When the distance is larger than ~300 km, the correlation coefficients of $N_{[10\text{-}30]}$ show a sudden drop, which may indicate that the NPF events have a typical spatial scale of several hundreds kilometers, consistent with a previous study (Birmili et al., 2013). The "source-driven" parameters eBC mass concentration

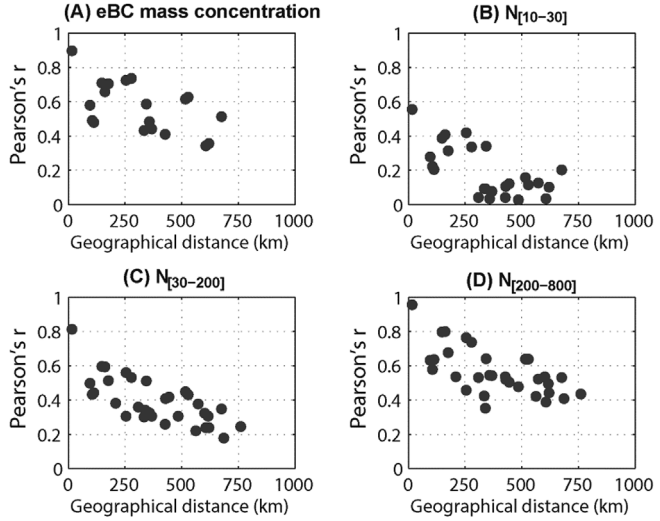

Fig. 8. Correlation coefficients of pollutant parameters of site pairs versus their geographical distance.

also shows a relatively high correlation even for a geographical distance larger than 500 km. Different from number concentrations, eBC mass concentration is a conserved parameter if there is no emission and scavenging. Therefore eBC mass concentration shows relatively high spatial homogeneity in a large area.

The analysis shown above provides an important reference for setting up an observation network with a specific research purpose. For example, to study the contribution of regional NPF to particle number concentration in different environments, sites in different categories should be set within a small area of 100–200 km; while for monitoring the regional background aerosol, a distance of ~500 km can be chosen between sites. Such an analysis may be also useful for the regional scale dispersion models and land use regression models.

5. Conclusion

Based on the long-term observation in German Ultrafine Aerosol Network (GUAN), the spatio-temporal variability of aerosol parameters including PNSD, PNCs and eBC mass concentration from 2009 to 2014 are investigated. Significant differences of pollutant concentration was observed between different site categories. Six-year median value of sub-micrometer PNC (diameter range 20–800 nm) varies between 900 cm^{-3} and 9000 cm^{-3}, while median eBC mass concentration varies between 0.1 and 2.3 $\mu g/m^3$.

A Spearman's rank correlation distance is applied to determine the similarity between observations in site pairs. PNCs in different size ranges were found to be with different spatial variabilities. Three size intervals are extracted: a higher spatial variability size range 10–30 nm, a transition size range 30–100 nm, and a lower spatial variability size range 100–800 nm.

A hierarchical clustering method was used to detect how pollutant parameters interfere with spatial characteristics. The results show that, the traditional "site category" (roadside, urban and regional background et al.) concerning mainly the influence of local anthropogenic sources cannot always catch the spatial distribution of aerosol particles. Parameters controlled by other processes may not show any difference between different site categories. For "source driven" pollutant parameters such as eBC mass concentration, the clustering result is basically in consistent with the traditional "site category", confirming that its spatial distribution is mainly determined by the distribution of anthropogenic emission sources, especially traffic sources. For pollutant parameters which are more influenced by long-range transport under certain meteorological conditions, such as $N_{[200\text{-}800]}$, the clustering result is highly connected with site locations, confirming that accumulation mode particles are distributed homogeneously in the background air in a large area.

To further investigate the spatial homogeneity of PNCs and eBC mass concentrations, the relationship between the similarity of measured parameters in site pairs and their geographical distance was analyzed. For all parameters, the correlation coefficient decreases with increasing geographical distance, which follows the "First Law of Geography". Different parameters show different sensitivities on geographical distance. The overall correlation coefficients of $N_{[200\text{-}800]}$ are highest among the parameters studied and well correlated with geographical distance. $N_{[10\text{-}30]}$ shows the lowest correlation coefficient due to the short lifetime of Young Aitken mode particles. And a sudden drop appears at a distance of ~300 km, indicating that NPF events may have a typical spatial scale of several hundred kilometers.

The long-term measurements in GUAN provides a valuable dataset to understand the spatial-temporal distributions of eBC mass concentration and particle number concentrations in Germany, and may be used in the regional scale dispersion models, land use regression models or epidemiological studies. The hierarchical clustering method used in this study offers a sound scientific base to compare pollutant parameters measured in different locations and environments and may be used to discover new "source clusters". It can be also used as an objective reference to check the validity of existing site classifications. Moreover, the analysis shown in this paper gives an important reference for setting up an observation network with a specific research purpose. For example, to study the contribution of regional NPF to particle number concentration in different environments, sites in different categories should be set within a small area of 100–200 km; while for monitoring the regional background aerosol, a distance of ~500 km can be chosen between sites.

Acknowledgement

We acknowledge funding by the German Federal Environment Ministry (BMU) grants F&E 370343200 (German title: Erfassung der Zahl feiner und ultrafeiner Partikel in der Außenluft) from 2008 to 2010, and F&E 371143232 (German title: Trendanalysen gesundheitsgefährdender Fein-und Ultrafeinstaubfraktionen unter Nutzung der im German Ultrafine Aerosol Network (GUAN) ermittelten Immissionsdaten durch Fortführung und Interpretation der Messreihen) from 2012 to 2014. For the Mülheim-Styrum measurements, we thank the co-funding by the North Rhine-Westphalia Agency for Nature, Environment and Consumer Protection (LANUV). Measurements at Annaberg-Buchholz were supported by the EU-Ziel3 project UltraSchwarz (German title: Ultrafeinstaub und Gesundheit im Erzgebirgskreis und Region Usti), grant 100083657. Measurements at Dresden-Winckelmannstraße were co-funded by the European Regional Development Fund Financing Programme Central Europe, grant No. 3CE288P (UFIREG). Measurements in Augsburg were granted by the Helmholtz-Zentrum München and partly by UFIREG (see above).

The authors would like to thank the technical and scientific staff members of the stations included in these analyses. André Sonntag and Stephan Nordmann (TROPOS) contributed to data processing. Prof. Dr. Thomas A.J. Kuhlbusch and Dr. Ulrich Quass contributed the data quality assurance and data analysis at Mülheim-Styrum. Horst-Günther Kath (State Dept. for Environmental and Agricultural Operations in Saxony, Betriebsgesellschaft für Umwelt und Landwirtschaft – BfUL), Andreas Hainsch (Labour Inspectorate of Lower Saxony, Staatliches Gewerbeaufsichtsamt Hildesheim – GAA), and Dieter Gladtke (Agency for Nature Protection, the Environment, and Customer Protection in Northrhine-Westfalia, Landesamt für Natur, Umwelt und Verbraucherschutz Nordrhein-Westfalen – LANUV) made the GUAN measurements possible at their respective observations sites.

This work was also accomplished in the frame of the project ACTRIS-2 (Aerosols, Clouds, and Trace gases Research InfraStructure)

under the European Union—Research Infrastructure Action in the frame of the H2020 program for "Integrating and opening existing national and regional research infrastructures of European interest" under Grant Agreement N654109 (H2020—Horizon 2020). Additionally, we acknowledge the WCCAP (World Calibration Centre for Aerosol Physics) as part of the WMO-GAW program base-funded by the German Environmental Agency (Umweltbundesamt).

Appendix A. Supplementary data

Supplementary data to this article can be found online at https://doi.org/10.1016/j.atmosenv.2018.12.029.

References

Asmi, A., Wiedensohler, A., Laj, P., Fjaeraa, A.M., Sellegri, K., Birmili, W., Weingartner, E., Baltensperger, U., Zdimal, V., Zikova, N., Putaud, J.P., 2011. Number size distributions and seasonality of submicron particles in Europe 2008–2009. Atmos. Chem. Phys. 11 (11), 5505–5538.

Asmi, A., Collaud Coen, M., Ogren, J.A., Andrews, E., Sheridan, P., Jefferson, A., Weingartner, E., Baltensperger, U., Bukowiecki, N., Lihavainen, H., Kivekäs, N., 2013. Aerosol decadal trends–Part 2: in-situ aerosol particle number concentrations at GAW and ACTRIS stations. Atmos. Chem. Phys. 13 (2), 895–916.

Barmpadimos, I., Hueglin, C., Keller, J., Henne, S., Prévôt, A.S.H., 2011. Influence of meteorology on PM 10 trends and variability in Switzerland from 1991 to 2008. Atmos. Chem. Phys. 11 (4), 1813–1835.

Beddows, D.C.S., Dall'Osto, M., Harrison, R.M., Kulmala, M., Asmi, A., Wiedensohler, A., Laj, P., Fjæraa, A.M., Sellegri, K., Birmili, W., Bukowiecki, N., 2014. Variations in tropospheric submicron particle size distributions across the European continent 2008–2009. Atmos. Chem. Phys. 14 (8), 4327–4348.

Beuck, H., Quass, U., Klemm, O., Kuhlbusch, T.A.J., 2011. Assessment of sea salt and mineral dust contributions to PM10 in NW Germany using tracer models and positive matrix factorization. Atmos. Environ. 45 (32), 5813–5821.

Bigi, A., Ghermandi, G., 2014. Long-term trend and variability of atmospheric PM_{10} concentration in the Po Valley. Atmos. Chem. Phys. 14 (10), 4895–4907.

Birmili, W., Wiedensohler, A., Heintzenberg, J., Lehmann, K., 2001. Atmospheric particle number size distribution in central Europe: statistical relations to air masses and meteorology. J. Geophys. Res.: Atmosphere 106 (D23), 32005–32018.

Birmili, W., Göbel, T., Sonntag, A., Ries, L., Sohmer, R., Gilge, S., Levin, I., Stohl, A., 2010. A case of transatlantic aerosol transport detected at the Schneefernerhaus Observatory (2650 m) on the northern edge of the Alps. Meteorol. Z. 19 (6), 591–600.

Birmili, W., Tomsche, L., Sonntag, A., Opelt, C., Weinhold, K., Nordmann, S., Schmidt, W., 2013. Variability of aerosol particles in the urban atmosphere of Dresden (Germany): effects of spatial scale and particle size. Meteorol. Z. 22 (2), 195–211.

Birmili, W., Sun, J., Weinhold, K., Merkel, M., Rasch, F., Spindler, G., Wiedensohler, A., Bastian, S., Loeschau, G., Schladitz, A., Quass, U., 2015. Atmospheric aerosol measurements in the German Ultrafine Aerosol Network (GUAN) Part 3: black Carbon mass and particle number concentrations 2009 to 2014. Gefahrst. Reinhalt. Luft 75 (11–12), 479–488.

Birmili, W., Weinhold, K., Rasch, F., Sonntag, A., Sun, J., Merkel, M., Wiedensohler, A., Bastian, S., Schladitz, A., Löschau, G., Cyrys, J., 2016. Long-term observations of tropospheric particle number size distributions and equivalent black carbon mass concentrations in the German Ultrafine Aerosol Network (GUAN). Earth Syst. Sci. Data 8 (2), 355.

Brüske, I., Hampel, R., Baumgärtner, Z., Rückerl, R., Greven, S., Koenig, W., Peters, A., Schneider, A., 2011. Ambient air pollution and lipoprotein-associated phospholipase A2 in survivors of myocardial infarction. Environ. Health Perspect. 119 (7), 921.

Butterfield, D., Beccaceci, S., Sweeney, B., Green, D., Alexander, J., Grieve, A., 2010. Annual Report for the UK Black Carbon Network. Nathonal Physical Laboratory, pp. 63.

Cavalli, F., Viana, M., Yttri, K.E., Genberg, J., Putaud, J.P., 2010. Toward a standardised thermal-optical protocol for measuring atmospheric organic and elemental carbon: the EUSAAR protocol. Atmos. Meas. Tech. 3 (1), 79–89.

Chen, X., Zhang, Z., Engling, G., Zhang, R., Tao, J., Lin, M., Sang, X., Chan, C., Li, S., Li, Y., 2014. Aerosol decadal trends–Part 1: characterization of fine particulate black carbon in Guangzhou, a megacity of South China. Atmos. Pollut. Res. 5 (3), 361–370.

Cheng, Y.H., Shiu, B.T., Lin, M.H., Yan, J.W., 2013. Levels of black carbon and their relationship with particle number levels—observation at an urban roadside in Taipei city. Environ. Sci. Pollut. Control Ser. 20 (3), 1537–1545.

Collaud Coen, M., Weingartner, E., Furger, M., Nyeki, S., Prévôt, A.S.H., Steinbacher, M., Baltensperger, U., 2011. Aerosol climatology and planetary boundary influence at the Jungfraujoch analyzed by synoptic weather types. Atmos. Chem. Phys. 11 (12), 5931–5944.

Collaud Coen, M., Andrews, E., Asmi, A., Baltensperger, U., Bukowiecki, N., Day, D., Fiebig, M., Fjæraa, A.M., Flentje, H., Hyvärinen, A., Jefferson, A., 2013. Aerosol decadal trends–Part 1: in-situ optical measurements at GAW and IMPROVE stations. Atmos. Chem. Phys. 13 (2), 869–894.

Collaud Coen, M., Praz, C., Haefele, A., Ruffieux, D., Kaufmann, P., Calpini, B., 2014. Determination and climatology of the planetary boundary layer height above the Swiss plateau by in situ and remote sensing measurements as well as by the COSMO-2 model. Atmos. Chem. Phys. 14 (23), 13205–13221.

Colvile, R.N., Hutchinson, E.J., Mindell, J.S., Warren, R.F., 2001. The transport sector as a source of air pollution. Atmos. Environ. 35 (9), 1537–1565.

Costabile, F., Birmili, W., Klose, S., Tuch, T., Wehner, B., Wiedensohler, A., Franck, U., König, K., Sonntag, A., 2009. Spatio-temporal variability and principal components of the particle number size distribution in an urban atmosphere. Atmos. Chem. Phys. 9 (9), 3163–3195.

Costabile, F., Amoroso, A., Wang, F., 2010. Sub-μm particle size distributions in a sub-urban Mediterranean area. Aerosol populations and their possible relationship with HONO mixing ratios. Atmos. Environ. 44 (39), 5258–5268.

Cyrys, J., Pitz, M., Heinrich, J., Wichmann, H.E., Peters, A., 2008. Spatial and temporal variation of particle number concentration in Augsburg, Germany. Sci. Total Environ. 401 (1–3), 168–175.

Di Ianni, A., Costabile, F., Barnaba, F., Di Liberto, L., Weinhold, K., Wiedensohler, A., Struckmeier, C., Drewnick, F., Gobbi, G.P., 2018. Black carbon aerosol in Rome (Italy): inference of a long-term (2001–2017) record and related trends from AERONET sun-photometry data. Atmosphere 9 (3), 81.

Dos Santos-Juusela, V., Petäjä, T., Kousa, A., Hämeri, K., 2013. Spatial–temporal variations of particle number concentrations between a busy street and the urban background. Atmos. Environ. 79, 324–333.

Engler, C., Rose, D., Wehner, B., Wiedensohler, A., Brüggemann, E., Gnauk, T., Spindler, G., Tuch, T., Birmili, W., 2007. Size distributions of non-volatile particle residuals (D $p < 800$ nm) at a rural site in Germany and relation to air mass origin. Atmos. Chem. Phys. 7 (22), 5785–5802.

Forrer, J., Rüttimann, R., Schneiter, D., Fischer, A., Buchmann, B., Hofer, P., 2000. Variability of trace gases at the high-Alpine site Jungfraujoch caused by meteorological transport processes. J. Geophys. Res.: Atmosphere 105 (D10), 12241–12251.

Griffiths, A.D., Conen, F., Weingartner, E., Zimmermann, L., Chambers, S.D., Williams, A.G., Steinbacher, M., 2014. Surface-to-mountaintop transport characterised by radon observations at the Jungfraujoch. Atmos. Chem. Phys. 14 (23), 12763–12779.

Hansen, J.E., Lacis, A.A., 1990. Sun and dust versus greenhouse gases: an assessment of their relative roles in global climate change. Nature 346 (6286), 713.

Harris, S.J., Maricq, M.M., 2001. Signature size distributions for diesel and gasoline engine exhaust particulate matter. J. Aerosol Sci. 32 (6), 749–764.

Hastie, T., Tibshirani, R., Friedman, J., 2009. Unsupervised learning. The Elements of Statistical Learning. Springer, New York, NY, pp. 485–585.

HEI, 2013. Understanding the health effects of ambient ultrafine particles. In: HEI Review Panel on Ultrafine Particles. HEI Perspectives 3. Health Effects Institute, Boston, Massachusetts, USA.

Henne, S., Brunner, D., Folini, D., Solberg, S., Klausen, J., Buchmann, B., 2010. Assessment of parameters describing representativeness of air quality in-situ measurement sites. Atmos. Chem. Phys. 10 (8), 3561–3581.

Hennig, F., Sugiri, D., Tzivian, L., Fuks, K., Moebus, S., Jöckel, K.H., Vienneau, D., Kuhlbusch, T.A., de Hoogh, K., Memmesheimer, M., Jakobs, H., 2016. Comparison of land-use regression modeling with dispersion and chemistry transport modeling to assign air pollution concentrations within the Ruhr area. Atmosphere 7 (3), 48.

Hitzenberger, R., Tohno, S., 2001. Comparison of black carbon (BC) aerosols in two urban areas–concentrations and size distributions. Atmos. Environ. 35 (12), 2153–2167.

Hofman, J., Staelens, J., Cordell, R., Stroobants, C., Zikova, N., Hama, S.M.L., Wyche, K.P., Kos, G.P.A., Van Der Zee, S., Smallbone, K.L., Weijers, E.P., Monks, P.S., Roekens, E., 2016. Ultrafine particles in four European urban environments: results from a new continuous long-term monitoring network. Atmos. Environ. 136, 68–81.

Jones, A.M., Harrison, R.M., Barratt, B., Fuller, G., 2012. A large reduction in airborne particle number concentrations at the time of the introduction of "sulphur free" diesel and the London low emission zone. Atmos. Environ. 50, 129–138.

King, B., 1967. Step-wise clustering procedures. J. Am. Stat. Assoc. 62 (317), 86–101.

Kreyling, W.G., Semmler-Behnke, M., Möller, W., 2006. Health implications of nanoparticles. J. Nanoparticle Res. 8 (5), 543–562.

Krudysz, M., Moore, K., Geller, M., Sioutas, C., Froines, J., 2009. Intra-community spatial variability of particulate matter size distributions in Southern California/Los Angeles. Atmos. Chem. Phys. 9 (3), 1061–1075.

Kruskal, W.H., 1958. Ordinal measures of association. J. Am. Stat. Assoc. 53 (284), 814–861.

Kulmala, M., Maso, M.D., Mäkelä, J.M., Pirjola, L., Väkevä, M., Aalto, P., Miikkulainen, P., Hämeri, K., O'dowd, C.D., 2001. On the formation, growth and composition of nucleation mode particles. Tellus B: Chem. Phys. Meteorol. 53 (4), 479–490.

Lanzinger, S., Schneider, A., Breitner, S., Stafoggia, M., Erzen, I., Dostal, M., Pastorkova, A., Bastian, S., Cyrys, J., Zscheppang, A., Kolodnitska, T., 2016. Ultrafine and fine particles and hospital admissions in Central Europe. results from the UFIREG study. Am. J. Respir. Crit. Care Med. 194 (10), 1233–1241.

Lugauer, M., Baltensperger, U., Furger, M., Gäggeler, H.W., Jost, D.T., Schwikowski, M., Wanner, H., 1998. Aerosol transport to the high Alpine sites Jungfraujoch (3454 m asl) and Colle Gnifetti (4452 m asl). Tellus B 50 (1), 76–92.

Lugauer, M., Baltensperger, U., Furger, M., Gäggeler, H.W., Jost, D.T., Nyeki, S., Schwikowski, M., 2000. Influences of vertical transport and scavenging on aerosol particle surface area and radon decay product concentrations at the Jungfraujoch (3454 m above sea level). J. Geophys. Res.: Atmosphere 105 (D15), 19869–19879.

Ma, N., Birmili, W., 2015. Estimating the contribution of photochemical particle formation to ultrafine particle number averages in an urban atmosphere. Sci. Total Environ. 512, 154–166.

Mikkonen, S., Korhonen, H., Romakkaniemi, S., Smith, J.N., Joutsensaari, J., Lehtinen, K.E.J., Hamed, A., Breider, T.J., Birmili, W., Spindler, G., Plass-Duelmer, C., 2011. Meteorological and trace gas factors affecting the number concentration of atmospheric Aitken (Dp = 50 nm) particles in the continental boundary layer: parameterization using a multivariate mixed effects model. Geosci. Model Dev. (GMD) 4 (1), 1.

Müller, T., Henzing, J.S., De Leeuw, G., Wiedensohler, A., Alastuey, A., Angelov, H.,

Bizjak, M., Collaud Coen, M., Engstrom, J.E., Gruening, C., Hillamo, R., 2011. Characterization and intercomparison of aerosol absorption photometers: result of two intercomparison workshops. Atmos. Meas. Tech. 4 (2), 245–268.
Murphy, D.M., Chow, J.C., Leibensperger, E.M., Malm, W.C., Pitchford, M., Schichtel, B.A., Watson, J.G., White, W.H., 2011. Decreases in elemental carbon and fine particle mass in the United States. Atmos. Chem. Phys. 11 (10), 4679–4686.
Myers, J.L., Well, A.D., Lorch, R.F., 2010. Research Design and Statistical Analysis. Routledge, New York.
Oberdörster, G., Elder, A., Rinderknecht, A., 2009. Nanoparticles and the brain: cause for concern? J. Nanosci. Nanotechnol. 9 (8), 4996–5007.
Olofson, K.F.G., Andersson, P.U., Hallquist, M., Ljungström, E., Tang, L., Chen, D., Pettersson, J.B., 2009. Urban aerosol evolution and particle formation during wintertime temperature inversions. Atmos. Environ. 43 (2), 340–346.
Pérez, N., Pey, J., Cusack, M., Reche, C., Querol, X., Alastuey, A., Viana, M., 2010. Variability of particle number, black carbon, and PM10, PM2. 5, and PM1 levels and speciation: influence of road traffic emissions on urban air quality. Aerosol Sci. Technol. 44 (7), 487–499.
Pfeifer, S., Birmili, W., Schladitz, A., Müller, T., Nowak, A., Wiedensohler, A., 2014. A fast and easy-to-implement inversion algorithm for mobility particle size spectrometers considering particle number size distribution information outside of the detection range. Atmos. Meas. Tech. 7 (1), 95–105.
Putaud, J.P., Van Dingenen, R., Alastuey, A., Bauer, H., Birmili, W., Cyrys, J., Flentje, H., Fuzzi, S., Gehrig, R., Hansson, H.C., Harrison, R.M., 2010. A European aerosol phenomenology–3: physical and chemical characteristics of particulate matter from 60 rural, urban, and kerbside sites across Europe. Atmos. Environ. 44 (10), 1308–1320.
Quass, U., Kuhlbusch, T., Koch, M., Fissan, H., Schmidt, K.G., Bruckmann, P., Pfeffer, U., Gladtke, D., Zang, T., 2004. Identification of Source Groups for Fine Dust. Public Report to the Environment Ministry of North Rhine Westphalia, Germany. pp. 12 IUTA-Report LP15/2004.
Rattigan, O.V., Civerolo, K., Doraiswamy, P., Felton, H.D., Hopke, P.K., 2013. Long term black carbon measurements at two urban locations in New York. Aerosol Air Qual. Res 13 (4), 1181–1196.
Reche, C., Querol, X., Alastuey, A., Viana, M., Pey, J., Moreno, T., Rodríguez, S., González, Y., Fernández-Camacho, R., Rosa, J., Dall'Osto, M., 2011. New considerations for PM, Black Carbon and particle number concentration for air quality monitoring across different European cities. Atmos. Chem. Phys. 11 (13), 6207–6227.
Rodríguez, S., Cuevas, E., 2007. The contributions of “minimum primary emissions” and “new particle formation enhancements” to the particle number concentration in urban air. J. Aerosol Sci. 38 (12), 1207–1219.
Rocach, L., Maimon, O., 2005. Clustering Methods Data Mining and Knowledge Discovery Handbook. Springer US, pp. 321.
Schmid, O., Stoeger, T., 2016. Surface area is the biologically most effective dose metric for acute nanoparticle toxicity in the lung. J. Aerosol Sci. 99, 133–143.
Spindler, G., Grüner, A., Müller, K., Schlimper, S., Herrmann, H., 2013. Long-term size-segregated particle (PM 10, PM 2.5, PM 1) characterization study at Melpitz–influence of air mass inflow, weather conditions and season. J. Atmos. Chem. 70 (2), 165–195.
Tobler, W.R., 1970. A computer movie simulating urban growth in the Detroit region. Econ. Geogr. 46 (Suppl. 1), 234–240.
Van Dingenen, R., Raes, F., Putaud, J.P., Baltensperger, U., Charron, A., Facchini, M.C., Decesari, S., Fuzzi, S., Gehrig, R., Hansson, H.C., Harrison, R.M., 2004. A European aerosol phenomenology—1: physical characteristics of particulate matter at kerbside, urban, rural and background sites in Europe. Atmos. Environ. 38 (16), 2561–2577.
van Pinxteren, D., Fomba, K.W., Spindler, G., Müller, K., Poulain, L., Iinuma, Y., Löschau, G., Hausmann, A., Herrmann, H., 2016. Regional air quality in Leipzig, Germany: detailed source apportionment of size-resolved aerosol particles and comparison with the year 2000. Faraday Discuss 189, 291–315.
von Bismarck-Osten, C., Birmili, W., Ketzel, M., Massling, A., Petäjä, T., Weber, S., 2013. Characterization of parameters influencing the spatio-temporal variability of urban particle number size distributions in four European cities. Atmos. Environ. 77, 415–429.
Wåhlin, P., Berkowicz, R., Palmgren, F., 2006. Characterisation of traffic-generated particulate matter in Copenhagen. Atmos. Environ. 40 (12), 2151–2159.
Wehner, B., Birmili, W., Gnauk, T., Wiedensohler, A., 2002. Particle number size distributions in a street canyon and their transformation into the urban-air background: measurements and a simple model study. Atmos. Environ. 36 (13), 2215–2223.
Wiedensohler, A., Birmili, W., Nowak, A., Sonntag, A., Weinhold, K., Merkel, M., Wehner, B., Tuch, T., Pfeifer, S., Fiebig, M., Fjæraa, A.M., 2012. Mobility particle size spectrometers: harmonization of technical standards and data structure to facilitate high quality long-term observations of atmospheric particle number size distributions. Atmos. Meas. Tech. 5, 657–685.
Wiedensohler, A., Wiesner, A., Weinhold, K., Birmili, W., Hermann, M., Merkel, M., Müller, T., Pfeifer, S., Schmidt, A., Tuch, T., Velarde, F., 2017. Mobility particle size spectrometers: calibration procedures and measurement uncertainties. Aerosol Sci. Technol. 1–19.
Wild, M., Gilgen, H., Roesch, A., Ohmura, A., Long, C.N., Dutton, E.G., Forgan, B., Kallis, A., Russak, V., Tsvetkov, A., 2005. From dimming to brightening: decadal changes in solar radiation at Earth's surface. Science 308 (5723), 847–850.
Winkler, P., 2009. Revision and necessary correction of the long-term temperature series of Hohenpeissenberg, 1781–2006. Theor. Appl. Climatol. 98 (3–4), 259–268.
WHO, (World Health Organization, European Office), 2012. Health Effects of Black Carbon. WHO, Copenhagen, Denmark.
Zanatta, M., Gysel, M., Bukowiecki, N., Müller, T., Weingartner, E., Areskoug, H., Fiebig, M., Yttri, K.E., Mihalopoulos, N., Kouvarakis, G., Beddows, D., 2016. A European aerosol phenomenology-5: climatology of black carbon optical properties at 9 regional background sites across Europe. Atmos. Environ. 145, 346–364.
Zíková, N., Ždímal, V., 2013. Long-term measurement of aerosol number size distributions at rural background station Košetice. Aerosol Air Qual. Res 13, 1464–1474.